Complexes of potentially tri- and tetra-dentate phosphinothiol ligands with Mo, W, Re, Fe, Ru, Os, Rh, Ir and Ni

Jonathan R. Dilworth,[a] Anthony J. Hutson,[a] Jason S. Lewis,[a] John R. Miller,[a] Yifan Zheng,[a] Qin Chen[b] and Jon Zubieta[b]

[a] *Department of Chemistry and Biological Chemistry, University of Essex, Wivenhoe Park, Colchester, Essex CO4 3SQ, UK*

[b] *Chemistry Department, Syracuse University, Syracuse, NY 13244, USA*

The phosphinothiolate proligand $PPh(C_6H_4SH-2)_2$ (H_2L^2) reacted with a variety of precursors to give the complexes $[ML^2_2]^{n-}$ (M = Mo, W or Re, n = 0; M = Fe, Ru, Os, Rh or Ir, n = 1). The crystal structure of the complex with M = Re revealed a distorted-octahedral geometry with the L^2 ligands facially co-ordinated. Other precursors gave the complexes $[ML^2_2X]^{n-}$ (X = Cl, M = Re, n = 0; X = NO, M = Mo, n = 1; M = Ru, n = 0; X = NR, M = Re, n = 1; X = NNMePh, M = Mo, n = 0; M = Ru, n = 1). The geometry of these seven-co-ordinate complexes is discussed. The metal(0) complexes $[M(CO)_3(MeCN)_3]$ (M = Mo or W) reacted with $[NMe_4]_2[L^2]$ to give orange $[NMe_4]_2[ML^2(CO)_3]$ the crystal structure of which (M = Mo) showed near-octahedral geometry with facially co-ordinated L^2. The complex $[IrCl(CO)(PPh_3)_2]$ reacted with H_2L^2 to give the iridium(III) hydride $[IrL^2(H)(CO)(PPh_3)]$. Its crystal structure showed the expected octahedral geometry with the H atom presumed to be *trans* to a thiolate sulfur. The potentially tetradentate ligand $P(C_6H_4SH-2)_3$ (H_3L^3) reacted with precursors containing Ru, Os and Rh to give $[M(HL^3)_2]^-$ (M = Ru, Os or Rh) where each HL^3 ligand is ligated *via* P and 2S with one unco-ordinated thiol group. These complexes were oxidised in air to give $[M(L^3)_2]^{n+}$ (M = Ru or Os, n = 0; M = Rh, n = 1) where L^3_2 is a hexadentate ligand formed by the coupling of two L^3 through two disulfide bonds.

Although metal complexes with tertiary phosphine or thiolate[1] ligands have been studied extensively, chelating phosphinothiolate ligands have received far less attention. The co-ordination chemistry of bidentate phosphinothiols has been explored to some extent,[2,3] but examples where they are potentially tri- or tetra-dentate are far less common.

The alkyl-bridged proligand $PPh(CH_2CH_2SH)_2$ (H_2L^1) has been shown to form complexes of the type $[MoL^1_2]^4$ and $[Mo(NNR_2)L^1_2]^4$ (R_2 = Ph_2 or MePh) and the rhenium complex $[ReL^1_2(L^1-P)]$ in which one SH group is not bound has been reported.[4] Block *et al.*[5] introduced a convenient new synthesis of the proligands $PPh(C_6H_4SH-2)_2$ (H_2L^2) and $P(C_6H_4SH-2)_3$ (H_3L^3), and the complex $[Mo(NNPh_2)L^2_2]$ was subsequently structurally characterised.[6] For the potentially tetradentate proligand H_3L^3 the isocyanide technetium complex $[TcL^3(CNPr^i)]$ has been prepared and structurally characterised.[7] The closely related rhenium complex $[ReL^3-(PPh_3)]$ has also been prepared.[8] There have been reports[9] of nickel complexes of L^3 and very recently the synthesis and structure of $[(FeL^3)_2S_2]$ was described.[10]

We here report an extensive investigation of the reactions of H_2L^2 and H_3L^3 with a range of precursors containing Mo, W, Re, Fe, Ru, Os, Rh and Ir.

Results and Discussion

Molybdenum and tungsten complexes

Analytical and selected spectroscopic data for the complexes discussed are summarised in Table 1.

(a) Syntheses and reactions of $[ML^2_2]$ (M = Mo 1 or W 2 and $[ML^2_2(MeCN)]$ (M = Mo 3 or W 4). Reaction of $[MCl_4(PPh_3)_2]$ with an excess of H_2L^2 in methanol under reflux gave the complexes $[ML^2_2]$ in good yield. These were isolated as air-stable brown (M = Mo 1) or green (M = W 2) solids that are stable in the solid state and soluble in a range of

H_2L^2

H_3L^3
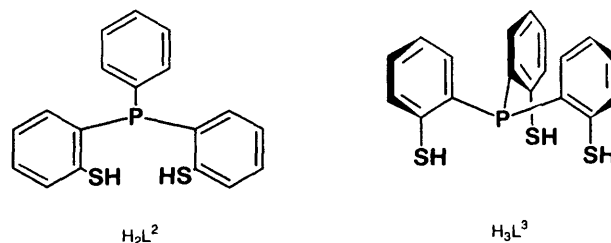
organic solvents. The complexes are diamagnetic in solution, and the ^1H NMR spectra show only multiplet resonances in the region δ 7–8 due to the phenyl groups. The ^{31}P NMR spectrum of the molybdenum complex **1** shows a singlet at δ 26.0 consistent with a structure involving equivalent P atoms. That of the tungsten complex **2** shows a comparable singlet at δ 30.1, but also doublets at δ 79.3 and 88.6 indicative of a possible mixture of species in solution. The singlets for the complexes are at comparatively high field, but there is no evidence from the FAB mass spectra (which shows m/z 833 for the tungsten complex with appropriate isotope distribution) for species with P=O bonds. In view of the P–P coupling the resonances at lower field are currently assigned to a second isomer with inequivalent P donors. However, we cannot entirely rule out the possibility that partial oxidation to the P=O ligand occurs in solution. The structure of the molybdenum complex is believed to be the same as that of $[ReL^2_2]$ which is discussed in detail below.

When the above synthetic reactions were carried out in acetonitrile air-stable complexes $[ML^2_2(NCMe)]$ (M = Mo **3** or W **4**) were isolated. The presence of ligated MeCN is confirmed by a strong IR band at about 2100 cm^{-1} and a singlet in the ^1H NMR with appropriate integration. The ^{31}P NMR spectra show singlets at δ 32.4 (M = Mo) and 36.3 (M = W), the difference in shifts from **1** and **2** showing that the MeCN is co-ordinated rather than being present as a molecule of

Table 1 Complexes of $PPh(C_6H_4SH\text{-}2)_2$ (H_2L^2) and $P(C_6H_4SH\text{-}2)_3$ (H_3L^3)

Complex	Colour	Elemental analyses[a] C	H	X	Principal IR[b] bands (cm⁻¹)	NMR (δ, J/Hz)[c] ¹H	³¹P	FAB mass spectrum,[d] m/z
1 $[MoL^2_2]$	Brown	58.4 (57.9)	3.3 (3.5)	S 16.8 (17.2)	—	7.6–7.0 (m, Ph)	26.0 (s)	746 (M^+)
2 $[WL^2_2]$	Green	51.7 (51.9)	3.2 (3.1)	S 15.2 (15.4)	—	7.8–7.0 (m, Ph)	30.1 (s)	833 ($M^+ + 1$)
3 $[MoL^2_2(NCMe)]$	Orange-brown	58.7 (58.1)	4.0 (3.7)	N 2.1 (1.7)	2100s [ν(C≡N)]	7.7–6.8 (m, 26 H, Ph), 1.8 (s, 3 H, CH₃CN)	32.4 (s)	—
4 $[WL^2_2(NCMe)]$	Dark green	52.6 (52.2)	3.4 (3.3)	N 1.2 (1.6)	2100s [ν(C≡N)]	7.7–7.0 (m, 26 H, Ph), 2.6 (s, 3 H, CH₃CN)	36.3 (s)	—
5 $[NMe_4]_2[MoL^2(CO)_3]$	Orange	53.0 (53.3)	5.7 (5.7)	N 4.4 (4.3)	1940, 1855, 1830 [ν(C≡O)]	7.1–6.5 (m, 13 H, Ph), 2.49 (s, 24 H, CH₃N)	28.3 (s)	—
6 $[NMe_4]_2[WL^2(CO)_3]$	Orange	46.6 (47.0)	4.9 (5.0)	N 3.7 (3.8)	1935, 1850, 1825, [ν(C≡O)]	7.9–6.4 (m, 13 H, Ph), 2.48	34.3 (s)	740 (M^+)
7 $[NMe_4]_2[Mo\{PMe\text{-}(C_6H_4S\text{-}2)_2\}(CO)_3]$	Orange	51.5 (51.3)	6.3 (6.3)	N 5.0 (5.0)	1940, 1860, 1830, [ν(C≡O)]	7.6–7.1 (m, 8 H, Ph), 1.5 (d, 3 H, CH₃P), 2.5 (s, 24 H, Me₄N)	6.4 (s)	—
8 $[\{NiL^2(PPh_3)\}_2]$	Green	53.0 (52.3)	5.7 (5.7)	—	—	7.7–6.8 (m, Ph)	26.9 (d), 87.2 (d), J(P–P) = 105.2	644 (M^+), 382 ($M^+ - PPh_3$)
9 $[MoL^2_2(CO)]$	Brown	57.7 (57.5)	4.0 (3.4)	S 16.6 (16.6)	1900s [ν(C≡O)]	7.7–6.8 (m, Ph)	29.1 (s)	774 (M^+), 746 ($M^+ - CO$)
10 $[NEt_3H][MoL^2_2(NO)]$	Brown-orange	55.8 (55.8)	3.3 (3.4)	N 1.6 (1.8)	1790s, [ν(N≡O)]	7.4–6.3 (m, Ph)	31 (d), 56 (s), J(P–P) = 63	776 (M^+), 746 ($M - NO$)
11 $[MoL^2_2(NNMePh)]$	Brown	55.7 (55.6)	3.8 (3.8)	N 3.0 (3.8)	1585 [ν(N=N)]	7.0–6.87 (m, 31 H, Ph), 5.4 (s, 2 H, CH₂Cl₂), 2.1 (s, 3 H, CH₃N)	86.2 (d), 96.4 (d), J(P–P) = 69	867 ($M^+ + 1$), 746 ($M^+ - NNMePh$)
12 $[WL^2_2(NNMe_2)]$	Dark green	50.9 (51.2)	3.4 (3.6)	N 2.9 (3.2)	1575m [ν(N=N)]	7.8–6.8 (m, 26 H, Ph), 1.6 (s, 3 H, CH₃N), 1.2 (s, 3 H, CH₃N)	74.1 (d), 82.3 (d), J(P–P) = 58	890 (M^+), 832 ($M^+ - NNMePh$), 845 (M^+)
13 $[ReL^2_2]$	Purple	52.1 (51.8)	3.1 (3.1)	S 15.3 (15.4)	—	e	28.4 (s)	...
14 $[ReL^2_2Cl]$	Purple	49.6 (49.7)	3.1 (3.0)	—	—	7.5–6.6 (m, Ph)		...
15 $[ReL^2_2(NNMePh)][BPh_4]$	Brown-orange	62.8 (63.1)	4.2 (4.3)	N 2.4 (2.2)	—	7.7–6.7 (m, 51 H, Ph) 3.3 (s, 3 H, NNMe)	37.2 (s)	—
16 $[PPh_4][ReL^2_2(NPh)]$	Green	62.5 (62.6)	4.2 (4.4)	N 1.1 (1.1)	—	7.7–6.8 (m, Ph)	26.2 (s, PPh₄), 31.5 (s, L²)	—
17 $[NEt_3H][FeL^2_2]$	Brown	61.1 (62.5)	5.1 (5.2)	N 1.6 (1.7)	—	e		—
18 $[NEt_3H][RuL^2_2]$	Brown	60.0 (59.2)	5.0 (5.0)	N 1.4 (1.6)	—	e		...
19 $[NEt_3H][OsL^2_2]$	Green	53.3 (53.6)	4.6 (4.5)	N 1.5 (1.5)	—	e		...

Compound	Colour	C	H	N	IR	^{1}H NMR	^{31}P NMR
20 [NEt$_4$][RuL^2$_2$]	Brown	60.3 (60.1)	5.5 (5.3)	N 1.4 (1.6)	—	e	—
21 [NEt$_4$][OsL^2$_2$]	Green	54.1 (54.5)	4.8 (4.8)	N 1.5 (1.4)	—	e	
22 [RuL^2$_2$(NO)]	Brown	55.1 (55.4)	4.6 (4.8)	N 1.6 (1.6)	1800, [ν(N≡O)]	e	—
23 [NEt$_3$H][RuL^2$_2$(CO)]	Yellow	58.3 (58.7)	4.6 (4.8)	N 1.6 (1.6)	1920, [ν(C≡O)]	e	—
24 [NEt$_3$H][Ru(HL^3)$_2$]·0.5CH$_2$Cl$_2$	Yellow	53.3 (53.6)	4.4 (4.4)	N 1.5 (1.6)	—	e	
25 [NEt$_3$H][Os(HL^3)$_2$]·0.5CH$_2$Cl$_2$	Green	48.8 (49.1)	4.0 (3.9)	N 1.2 (1.3)	—	e	—
26 [Ru(L^3$_2$)]·CH$_2$Cl$_2$	Brown	49.6 (49.6)	2.9 (3.0)	—	—	8.3–6.6 (m, 24 H, Ph), 5.3 (s, 2 H, CH$_2$Cl$_2$)	98.7 (s)
27 [Os(L^3$_2$)]·CH$_2$Cl$_2$	Brown	45.2 (45.1)	2.9 (2.7)	—	—	7.9–6.7 (m, 24 H, Ph), 5.3 (s, 2 H, CH$_2$Cl$_2$)	71.9 (s)
28 [RuL^3(NO)(PPh$_3$)]	Brown	56.7 (57.7)	4.6 (4.8)	N 1.8 1.9	1812, [ν(N≡O)]	7.8–6.3 (m, Ph)	111.9 (d), 25.9 (d), J(P–P) = 260
29 [{RuL^3(CO)(PPh$_3$)}$_n$]	Yellow	58.7 (59.5)	3.8 (3.6)	—	1955, [ν(C≡O)]	f	—
30 [NEt$_3$H][RhL^2$_2$]	Orange	58.5 (59.1)	4.8 (5.0)	N 1.5 (1.5)	—	f	
31 [NEt$_3$H][IrL^2$_2$]	Yellow	53.8 (53.5)	4.8 (4.4)	N 1.3 (1.5)	—	f	
32 [NBu^n$_4$][RhL^2$_2$]	Orange	63.2 (62.8)	6.2 (6.3)	N 1.3 (1.4)	—	7.7–6.6 (m, 26 H, Ph), 3.19 (t, 8 H, CH$_3$CH$_2$CH$_2$CH$_2$), 1.65 (m, 8 H, CH$_3$CH$_2$CH$_2$CH$_2$), 1.18 (m, 8 H, CH$_3$CH$_2$CH$_2$CH$_2$), 0.87 (t, 12 H, CH$_3$CH$_2$)	—
33 [NBu^n$_4$][IrL^2$_2$]	Yellow	57.5 (57.6)	5.7 (5.8)	N 1.3 1.4	—	7.8–6.5 (m, 26 H, Ph) 3.19 (t, 8 H, CH$_3$CH$_2$CH$_2$CH$_2$), 1.65 (m, 8 H, CH$_3$CH$_2$CH$_2$CH$_2$), 1.18 (m, 8 H, CH$_3$CH$_2$CH$_2$CH$_2$), 0.87 (t, 12 H, CH$_3$CH$_2$CH$_2$CH$_2$)	48.0 (s)
34 [IrL^2(H)(CO)(PPh$_3$)]	White	55.5 (55.1)	3.3 (3.5)	—	2110w [ν(Ir–H)], 2032s, [ν(C≡O)]	7.7–6.3 (m, Ph), −11.34 [t, 1rH, J(P–H) = 11.7]	—
35 [Ir(HL^3)H(CO)(PPh$_3$)]	White	52.3 (52.9)	3.5 (3.5)	—	2567w [ν(S–H)], 2110w - [ν(Ir–H)], 2032s [ν(C≡O)]	7.7–6.4 (m, 30 H, Ph), −10.6 [t, 1 H, Ir–H, J(P–H) = 11.7]	6.2 (d), 57.0 (d), J(P–P) = 299
36 [NEt$_3$H][Rh(HL^3)$_2$]	Yellow	54.4 (55.0)	4.6 (4.6)	N 1.5 (1.5)	2587w [ν(S–H)]	0.76 [t, 9 H, CH$_3$CH$_2$), 2.64 (q, 6 H, CH$_3$CH$_2$), 4.31 (s, 2 H, SH), 8.0–6.4 (m, 24 H, Ph)	83.3 (d), J(Rh–P) = 107.3
37 [Rh(L^2$_2$)]Cl	Orange	50.3 (50.9)	3.1 (2.9)	—	—	7.9–6.6 (m, Ph)	87.3 (d), J(Rh–P) = 94.0

^{a} Calculated values in parentheses. ^{b} Recorded as Nujol mulls; s = strong, w = weak. ^{c} Recorded in CDCl$_3$ solution. ^{d} Most intense peak reported. ^{e} Paramagnetic. ^{f} Insoluble.
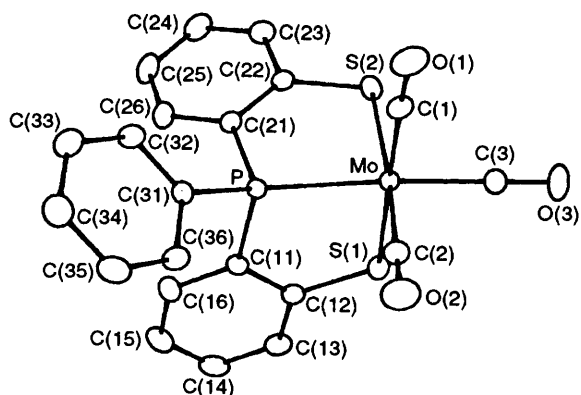
Fig. 1 An ORTEP[12] view of the structure of the anion of [NMe₄]₂[MoL²(CO)₃] with the atom labelling scheme

Table 2 Fractional coordinates for [NMe]₂[MoL²(CO)₃] **5**

Atom	x	y	z
Mo	0.027 63(3)	0.223 39(2)	0.134 90(2)
S(1)	−0.015 5(1)	0.262 79(6)	0.272 40(6)
S(2)	−0.135 35(9)	0.113 94(5)	0.133 70(6)
P	−0.192 49(8)	0.288 66(5)	0.097 81(5)
O(1)	0.081 9(3)	0.170 6(2)	−0.026 6(2)
O(2)	0.207 3(3)	0.356 4(2)	0.106 9(2)
O(3)	0.285 7(3)	0.136 2(2)	0.216 6(2)
N(1)	0.637 9(3)	0.152 7(2)	0.345 3(2)
N(2)	0.774 3(3)	0.079 8(2)	0.849 3(2)
C(1)	0.058 4(4)	0.190 4(2)	0.033 1(2)
C(2)	0.139 2(4)	0.307 5(2)	0.122 1(2)
C(3)	0.188 9(3)	0.168 3(2)	0.185 9(2)
C(11)	−0.222 3(3)	0.345 2(2)	0.181 0(2)
C(12)	−0.143 9(4)	0.329 3(2)	0.257 0(2)
C(13)	−0.172 2(4)	0.368 2(2)	0.322 0(2)
C(14)	−0.273 5(4)	0.420 4(2)	0.313 1(3)
C(15)	−0.348 5(4)	0.436 1(2)	0.238 5(3)
C(16)	−0.324 5(4)	0.399 0(2)	0.173 6(2)
C(21)	−0.332 4(3)	0.222 4(2)	0.085 2(2)
C(22)	−0.300 1(3)	0.147 3(2)	0.099 4(2)
C(23)	−0.408 4(4)	0.096 4(2)	0.087 0(3)
C(24)	−0.539 4(4)	0.119 6(3)	0.065 4(3)
C(25)	−0.570 6(4)	0.193 9(3)	0.055 2(3)
C(26)	−0.467 3(4)	0.244 5(2)	0.064 5(2)
C(31)	−0.237 2(3)	0.353 9(2)	0.015 0(2)
C(32)	−0.328 6(4)	0.340 0(2)	−0.055 4(2)
C(33)	−0.358 1(4)	0.393 5(2)	−0.115 0(2)
C(34)	−0.295 2(5)	0.460 8(2)	−0.104 0(2)
C(35)	−0.200 4(4)	0.474 7(2)	−0.035 9(2)
C(36)	−0.169 3(4)	0.422 0(2)	0.022 5(2)
C(41)	0.604 0(5)	0.212 2(3)	0.284 6(3)
C(42)	0.529 8(5)	0.144 8(4)	0.389 1(3)
C(43)	0.652 3(8)	0.083 0(3)	0.304 3(4)
C(44)	0.764 8(5)	0.172 3(5)	0.401 8(4)
C(51)	0.877 2(5)	0.022 9(3)	0.877 1(4)
C(52)	0.658 0(5)	0.048 1(3)	0.790 2(3)
C(53)	0.724 1(5)	0.111 4(4)	0.916 3(3)
C(54)	0.834 4(5)	0.140 5(3)	0.807 7(3)

Table 3 Selected bond lengths (Å) and angles (°) for complex **5**

Mo–S(1)	2.591(1)	O(3)–C(3)	1.164(4)
Mo–S(2)	2.575(1)	C(11)–C(12)	1.405(5)
Mo–P	2.4830(9)	C(11)–C(16)	1.408(5)
Mo–C(1)	1.934(4)	C(12)–C(13)	1.399(5)
Mo–C(2)	1.935(4)	C(13)–C(14)	1.380(6)
Mo–C(3)	1.954(4)	C(14)–C(15)	1.372(6)
S(1)–C(12)	1.750(4)	C(15)–C(16)	1.366(6)
S(2)–C(22)	1.754(4)	C(21)–C(22)	1.407(5)
P–C(11)	1.834(4)	C(21)–C(26)	1.395(5)
P–C(21)	1.833(4)	C(22)–C(23)	1.413(5)
P–C(31)	1.828(4)	C(23)–C(24)	1.365(6)
O(1)–C(1)	1.156(5)	C(24)–C(25)	1.384(6)
O(2)–C(2)	1.185(5)	C(25)–C(26)	1.372(6)
S(1)–Mo–S(2)	89.22(4)	Mo–C(1)–O(1)	177.5(3)
S(1)–Mo–P	77.66(3)	Mo–C(2)–O(2)	173.6(4)
S(1)–Mo–C(1)	178.0(1)	Mo–C(3)–O(3)	179.3(4)
S(1)–Mo–C(2)	95.9(1)	P–C(11)–C(12)	117.1(3)
S(1)–Mo–C(3)	91.1(1)	P–C(11)–C(16)	123.7(3)
S(2)–Mo–P	79.90(3)	C(12)–C(11)–C(16)	119.0(3)
S(2)–Mo–C(1)	89.0(1)	S(1)–C(12)–C(11)	122.4(3)
S(2)–Mo–C(2)	172.9(1)	S(1)–C(12)–C(13)	119.8(3)
S(2)–Mo–C(3)	94.9(1)	C(11)–C(12)–C(13)	117.8(4)
P–Mo–C(1)	102.9(1)	C(12)–C(13)–C(14)	122.0(4)
P–Mo–C(2)	96.4(1)	C(13)–C(14)–C(15)	119.7(4)
P–Mo–C(3)	167.6(1)	C(14)–C(15)–C(16)	120.1(4)
C(1)–Mo–C(2)	85.9(2)	C(11)–C(16)–C(15)	121.3(4)
C(1)–Mo–C(3)	88.1(2)	P–C(21)–C(22)	117.7(3)
C(2)–Mo–C(3)	89.9(2)	P–C(21)–C(26)	122.3(3)
Mo–S(1)–C(12)	108.4(1)	C(22)–C(21)–C(26)	119.9(3)
Mo–S(2)–C(22)	107.5(1)	S(2)–C(22)–C(21)	124.1(3)
Mo–P–C(11)	110.7(1)	S(2)–C(22)–C(23)	118.6(3)
Mo–P–C(21)	110.4(1)	C(21)–C(22)–C(23)	117.3(3)
Mo–P–C(31)	124.5(1)	C(22)–C(23)–C(24)	121.3(4)
C(11)–P–C(21)	101.8(2)	C(23)–C(24)–C(25)	121.0(4)
C(11)–P–C(31)	101.0(2)	C(24)–C(25)–C(26)	119.0(4)
C(21)–P–C(31)	105.8(2)	C(21)–C(26)–C(25)	121.4(4)

crystallisation. The structures of these complexes are presumed to be analogous to that of the carbonyl complex discussed below.

Attempts to generate hydride complexes by reaction with stoichiometric amounts of HBF₄·Et₂O were unsuccessful, and led to extensive decomposition. The results of studies of the electrochemical oxidation and reduction of these complexes and others reported in the paper will be given elsewhere.

(b) Synthesis, crystal structure and reactions of [NMe₄]₂-[MoL²(CO)₃] 5. The molybdenum(0) precursor [Mo(CO)₃(N-CMe)₃] reacts readily with [NMe₄]₂[L²] to give the orange complex [NMe₄]₂[MoL²(CO)₃] **5** in good yield. This is directly analogous to [NMe₄]₂[MoL¹(CO)₃] which was

prepared in a similar manner.[11] The related tungsten complex [NMe₄]₂[WL²(CO)₃] **6** and [NMe₄]₂[Mo{PMe(C₆H₄S-2)₂}(CO)₃] **7** were synthesised similarly using appropriate precursors. The complexes were isolated as extremely oxygen-sensitive orange (Mo) or yellow (W) solids. These had unexceptional ¹H NMR spectra with broad multiplets in the δ 6–7 region assigned to the phosphine phenyl groups except for **7** which showed a doublet due to the phosphorus-bound methyl group. All these complexes showed a sharp singlet in their ³¹P NMR spectra due to the single co-ordinated P atom. The IR spectra as Nujol mulls showed two strong bands in the region 1900–2000 cm⁻¹ assigned to ν(C≡O).

Orange prisms of [NMe₄]₂[MoL²(CO)₃] **5** suitable for a crystal structure determination were obtained by slow cooling of the reaction mixture.

Structure of the anion [MoL²(CO)₃]²⁻ **5**. A representation of the structure appears in Fig. 1 together with the atom numbering scheme. Atomic coordinates are given in Table 2 and selected bond lengths and angles in Table 3. The geometry about the Mo is distorted octahedral, with an approximate plane of symmetry containing the C(3)–Mo–P plane. The Mo–CO bond distances are normal [1.934(4)–1.954(4) Å] and lie close to the values for [Mo(CO)₆]. Due to the constraints of the P–C–C–S chelate rings the S–Mo–P bond angles are significantly reduced from the ideal octahedral values of 90° to 77.66(3) and 79.90(3)°. The L² ligand occupies one face of the octahedron.

Reactions of [ML²(CO)₃]²⁻. We have previously shown that the dianion [MoL¹(CO)₃]²⁻ reacts readily with 1,2-dihalo-genoethanes in a template reaction to give the molybdenum(0) tricarbonyl complex of a macrocycle.[11] However, despite repeated attempts, we have been unable to generate an analogous dibenzo macrocycle from [MoL²(CO)₃]²⁻. At-

tempts at the template reaction with 1,3-dibromopropane and $C_6H_4(CH_2Cl)_2$-1,2 also failed, and no characterisable products could be obtained. The lack of macrocycle formation may reflect the relatively lower basicity of the arene sulfurs, and/or the unfavourable configuration of the dibenzo macrocyclic ring.

However, surprisingly, the dianion $[MoL^2(CO)_3]^{2-}$ reacted readily with $NiCl_2$ in dry acetonitrile to give a pale green air-stable complex analysing as $[NiL^2(PPh_3)]$ **8**. The formation of this species was surprising, as we had expected a binuclear complex with thiolates bridging between nickel and molybdenum. It appears that reaction of the molybdenum dianion with Ni destabilises the complex sufficiently for transfer of the PS_2 ligand from Mo to Ni. This transfer may well be facilitated by the acetonitrile solvent co-ordinating to the Mo. The new complex gave the expected ion at m/z 644 with appropriate isotope distribution, and the ^{31}P NMR spectrum exhibits two doublets at δ 26.9 and 87.2 due to the two inequivalent phosphorus atoms.

The diamagnetism of the complex would be consistent with square-planar geometry but, as the structure of the $[MoL^2(CO)_3]^{2-}$ anion shows, L^2 generally prefers to occupy three facial sites of an octahedron. The structure of $[Mo(NNMePh)L^2{}_2]$ discussed below shows that although near-planar co-ordination of L^2 is possible it has so far only been observed for the equatorial sites in pentagonal-bipyramidal co-ordination where the small bite angle of the ligand can be accommodated. Thiolate bridging could generate higher co-ordination numbers, and since most five-co-ordinate nickel(II) complexes are diamagnetic the structure **A** is a possibility. In view of the observation of the molecular ion for $[NiL^2(PPh_3)]$, and no higher oligomers, dissociation presumably occurs in the mass spectrometer.

(c) **Synthesis of $[MoL^2{}_2(CO)]$ 9.** Despite several attempts no clean products could be isolated from the reaction of $[MoCl_2(CO)_4]$ with H_2L^2 in a variety of solvents. The insolubility of the products in a range of organic solvents suggested that they are probably polymeric with thiolate bridges. However $[MoCl_2(CO)_2(PPh_3)_2]$ reacted smoothly with H_2L^2 in methanol in the presence of base to give an air-stable brick-red solid analysing as $[MoL^2{}_2(CO)]$ **9**. This complex has a strong IR band at 1900 cm^{-1} (Nujol mull) and the ^{31}P NMR spectrum shows a singlet at δ 29.1, consistent with equivalent P atoms. The FAB mass spectrum shows ions at m/z 774 and 746 assignable to $[MoL^2{}_2(CO)]^+$ and $[MoL^2{}_2]^+$ respectively. Both have the appropriate isotope distribution patterns. Reaction of $[MoL^2{}_2]$ **1** with CO at atmospheric pressure in dichloromethane gives a dark solution with a strong IR band at 1880 cm^{-1} (1860 for M = W) assigned to $v(C\equiv O)$. However, work-up of these solutions gave intractable oils. Unfortunately we were unable to obtain X-ray-quality crystals of the monocarbonyl species, and we ascribe the difference in stability to the formation of different isomers *via* the two different preparative routes. A variety of structures including pentagonal prismatic and capped octahedral are possible but cannot be distinguished in the absence of X-ray structural data. However, the equivalence of the P atoms shown by the ^{31}P NMR spectra confirms that the structure cannot be analogous to that of complex **10** below as this has inequivalent phosphorus ligands. One possibility is co-ordination of the CO such that it bisects both P–Re–P and S–Re–S angles to give a symmetrical structure with equivalent P atoms.

Stable thiolatocarbonyl complexes of Mo^{IV} are rare, and the only other reported examples are $[Mo(CO)_2L'_2]$ (L' = 4,6-di-*tert*-butylbenzene-1,2-dithiol)[13] and $[Mo(CO)(PR_3)L'_2]$ (PR$_3$ = PPh$_3$ or PMe$_3$). The IR bands for $v(C\equiv O)$ in the phosphine-substituted complexes are 1968 (PMe$_3$) or 1978 cm^{-1} (PPh$_3$), which compare well with the values found for our complex. The structure of $[Mo(CO)(PPh_3)L'_2]$ was analysed in
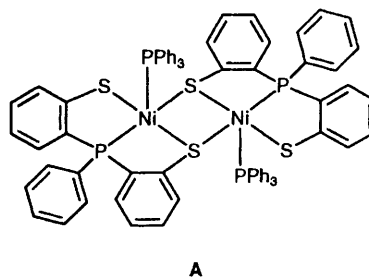
A

detail for evidence of S···S interactions which would effectively reduce the formal oxidation state of the metal. It was concluded[13] that these were not significant, and we likewise believe that $[MoL^2{}_2(CO)]$ contains molybdenum in the quadrivalent state.

Synthesis and properties of $[NEt_3H][MoL^2{}_2(NO)]$ 10. Reaction of $[NEt_3H][Mo(SPh)_4(NO)]$[14] with 2 equivalents of H_2L^2 in methanol under reflux in the presence of NEt$_3$ gave $[NEt_3H][MoL^2{}_2(NO)]$ **10** as an air-stable brown-orange solid. This complex exhibited a strong IR band at 1790 cm^{-1} due to co-ordinated NO and the observation of two doublets in the ^{31}P NMR spectrum suggested a structure with inequivalent P atoms different to that of the carbonyl complex. The NO ligand is almost certainly bonded in a linear mode conferring a formal valence-electron count of 18. The FAB mass spectrum showed a strong ion at m/z 776 (M^+) and an ion corresponding to $[MoL^2{}_2]^+$ at m/z 746. Both had the expected isotope distribution patterns.

The polymeric species $[Mo(NO)(H_2NO)_2(H_2O)_n]$[15] reacts readily with an excess of benzenethiolate anion to give the red nitrosyl thiolate anion $[Mo(SPh)_4(NO)]^-$.[14] Reaction of this species with H_2L^2 gave an intense purple solid which showed a strong IR band at 1770 cm^{-1} due to $v(NO)$ and bands ascribable to the phosphinothiolate ligand. However this could not be satisfactorily characterised and the observation of several peaks in the ^{31}P NMR spectrum suggested a mixture.

Synthesis and properties of $[ML^2{}_2(NNR_2)](R_2$ = MePh; M = Mo 11; R_2 = Me$_2$, M = W 12. Reaction of the complexes $[MCl(NNR_2)_2(PPh_3)_2]Cl$[16] (M = W; R_2 = Me$_2$; M = Mo, R_2 = MePh) with H_2L^2 in methanol gave the complexes $[ML^2{}_2(NNR_2)]$ as brown (M = Mo 11) or green (M = W 12) air-stable solids. The ^1H NMR spectrum of the tungsten complex shows two singlets at δ 1.2 and 1.6 due to inequivalent hydrazido methyl groups. The P donors are also inequivalent, as shown by the appearance of two doublets at δ 74.1 and 82.3 $[J(P–P) = 58$ Hz]. The FAB mass spectrum shows an ion at m/z 890 and one at m/z 832 due to the $[WL^2{}_2]^+$ ion formed by loss of the NNMe$_2$ ligand. Both peak clusters had appropriate isotope distributions.

For complex **11** the hydrazide methyl appears as the expected singlet in the ^1H NMR spectrum and the ^{31}P NMR spectrum shows two doublets indicating inequivalent P donor atoms. The FAB mass spectrum shows an $[M + 1]^+$ ion at m/z 867 and a peak at m/z 746 corresponding to $[MoL^2{}_2]^+$ again with appropriate isotope distributions.

Crystal structure of complex **11.** We have made a brief earlier report[6] of the structure of complex **11** and here confine ourselves to a more detailed discussion. An ORTEP picture of the structure with a partial atom-labelling scheme appears in Fig. 2. The geometry about Mo is significantly distorted from pentagonal bipyramidal due largely to the small bite angle of the phosphinothiolate ligands. The most striking feature is that while the P(1)S(1)S(2) ligand spans equatorial and axial sites, the P(2)S(4)S(6) ligand lies in three equatorial sites. The latter is an unprecedented mode of co-ordination for L^2 which normally occupies a facial site in octahedral complexes; *mer* co-ordination is presumably possible in this situation as the

**Table 4** Fractional coordinates for [ReL^2$_2$]·Et$_2$O 13

Atom	x	y	z	Atom	x	y	z
Re(1)	0.75	0.364 41(2)	1.0	Re(2)	0.75	0.652 12(2)	0.5
S(1)	0.752 77(7)	0.208 47(9)	0.918 08(6)	S(3)	0.718 79(6)	0.699 7(1)	0.377 18(5)
S(2)	0.627 41(5)	0.409 6(1)	0.991 07(5)	S(4)	0.838 73(6)	0.496 22(9)	0.525 85(6)
P(1)	0.724 93(5)	0.493 39(8)	0.895 15(5)	P(2)	0.854 12(5)	0.779 27(8)	0.503 79(5)
C(11)	0.746 5(2)	0.405 0(4)	0.823 9(2)	C(41)	0.936 8(2)	0.692 8(4)	0.548 6(2)
C(12)	0.756 0(2)	0.277 7(4)	0.836 3(2)	C(42)	0.927 1(2)	0.564 6(4)	0.556 1(2)
C(13)	0.766 6(2)	0.202 2(4)	0.781 3(2)	C(43)	0.988 1(2)	0.491 3(4)	0.586 2(2)
C(14)	0.768 5(3)	0.253 7(5)	0.716 8(2)	C(44)	1.057 3(2)	0.541 8(5)	0.608 5(2)
C(15)	0.761 4(2)	0.378 4(5)	0.705 8(2)	C(45)	1.066 9(3)	0.668 2(5)	0.602 4(3)
C(16)	0.749 9(2)	0.454 0(4)	0.759 1(2)	C(46)	1.006 8(2)	0.743 3(4)	0.572 0(2)
C(21)	0.768 2(2)	0.643 3(3)	0.896 1(2)	C(51)	0.866 4(2)	0.933 6(3)	0.543 8(2)
C(22)	0.837 5(2)	0.654 5(4)	0.886 2(3)	C(52)	0.844 6(2)	1.037 4(4)	0.501 4(2)
C(23)	0.871 2(3)	0.770 3(5)	0.892 0(3)	C(53)	0.850 8(3)	1.154 8(4)	0.531 8(3)
C(24)	0.835 7(3)	0.873 4(4)	0.907 3(3)	C(54)	0.877 9(2)	1.167 5(4)	0.604 8(3)
C(25)	0.768 0(3)	0.863 0(4)	0.916 9(3)	C(55)	0.898 0(2)	1.066 2(5)	0.648 0(2)
C(26)	0.734 5(2)	0.749 1(4)	0.912 3(2)	C(56)	0.892 4(2)	0.949 0(4)	0.617 6(2)
C(31)	0.627 5(2)	0.527 1(4)	0.864 3(2)	C(61)	0.856 1(2)	0.808 8(3)	0.412 4(2)
C(32)	0.586 9(2)	0.493 6(4)	0.910 9(2)	C(62)	0.792 0(2)	0.781 6(3)	0.358 5(2)
C(33)	0.512 7(2)	0.522 5(5)	0.893 4(3)	C(63)	0.784 7(3)	0.818 1(4)	0.288 0(2)
C(34)	0.478 4(3)	0.580 7(6)	0.829 4(3)	C(64)	0.842 2(3)	0.876 6(5)	0.271 6(2)
C(35)	0.517 4(3)	0.610 7(6)	0.781 6(3)	C(65)	0.907 2(2)	0.899 9(5)	0.324 0(2)
C(36)	0.592 0(2)	0.587 2(4)	0.800 0(2)	C(66)	0.913 9(2)	0.867 8(4)	0.394 2(2)
O	0.484 7(4)	0.945 5(7)	0.166 8(3)	C(3)	0.494 8(7)	1.109(1)	0.098 0(6)
C(1)	0.447 9(6)	0.847(1)	0.177 2(6)	C(4)	0.476 7(6)	0.773(1)	0.223 5(5)
C(2)	0.457 2(7)	1.023(1)	0.112 7(6)				
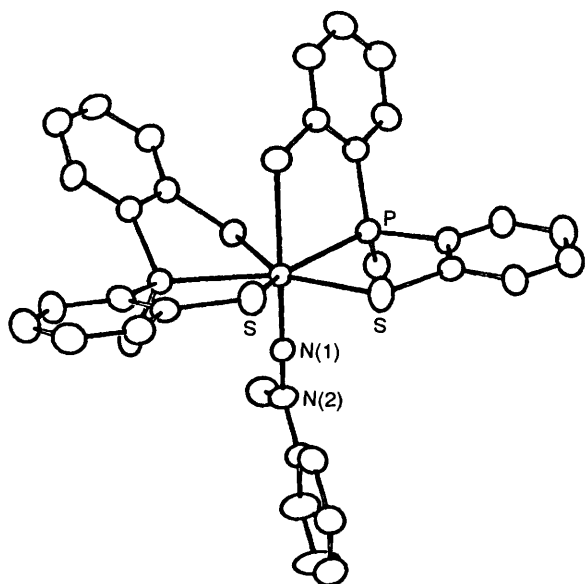
Fig. 2 An ORTEP view of the structure of [MoL^2$_2$(NNMePh)]

equatorial sites of the pentagonal bipyramid can accommodate the small ligand bite angles. The two distinct co-ordination modes for the two L^2 ligands are entirely consistent with the observed inequivalence of the P atoms in the ^{31}P NMR spectrum. The tungsten complex **12** presumably has the same structure.

Rhenium complexes

Synthesis and properties of [ReL^2$_2$] 13. Reaction of [ReOCl$_3$(PPh$_3$)$_2$] or [ReOCl$_4$]$^-$ with 2 equivalents of H$_2$L^2 in methanol under reflux gave [ReL^2$_2$] **13** as a purple air-stable solid in high yield. The complex is paramagnetic, as expected for a rhenium(IV) d^3 system and only very broad solution NMR spectra were observed. The complex shows an ion at m/z 845 with the appropriate isotope splitting pattern. Suitable crystals of a diethyl ether solvate were grown from dichloromethane–diethyl ether and a crystal structure determination was carried out.
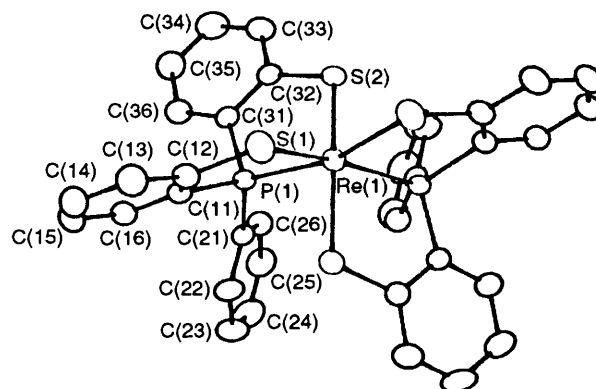
Fig. 3 An ORTEP view of one of the two molecules of [ReL^2$_2$] with the atom labelling scheme

Crystal structure of complex **13**. A view of the structure of one of the two independent molecules is shown in Fig. 3, together with the atom-labelling scheme. Atomic co-ordinates are given in Table 4 and selected bond lengths and angles in Table 5. There are two independent and very similar molecules in the unit cell and the dimensions of both are shown. The Re atoms lie on crystallographic two-fold axes. The geometry about the Re is best described as distorted octahedral with the two P donors in a *cis* configuration. The principal distortions are the result of the bite angles of the ligands (*ca.* 82–83 °C) and steric repulsion between the phosphine groups which opens up the P(1)–Re–P(1') angle to 108.8(1)°. Both tridentate PS$_2$ ligands are bound in a facial manner, and molecular models confirm that they are unable to span meridional sites of an octahedron without substantial distortion due to the pyramidal co-ordination of phosphorus. The Re–S and Re–P distances are unremarkable and close to values found for other phosphino-thiolate ligands.

The formation of paramagnetic [ReL^2$_2$] is in marked contrast to analogous reactions with PPh(CH$_2$CH$_2$SH)$_2$ (L^1) which produced an orange *diamagnetic* complex, analysing as the rhenium(III) complex [ReL^1$_2$].[4] However, all four thiolates could not be ligated as monoanionic donors or the formal oxidation would be 4 and we assigned the structure as a five-

Table 5 Selected bond lengths (Å) and angles (°) for complex 13

Re(1)–S(1)	2.327(1)	Re(2)–S(4)	2.329(1)
Re(1)–S(1')	2.327(1)	Re(2)–S(4')	2.329(1)
Re(1)–S(2)	2.331(1)	Re(2)–S(3)	2.337(1)
Re(1)–S(2')	2.331(1)	Re(2)–S(3')	2.337(1)
Re(1)–P(1)	2.395(1)	Re(2)–P(2)	2.388(1)
Re(1)–P(1')	2.395(1)	Re(2)–P(2')	2.388(1)
S(1)–Re(1)–S(1')	87.19(6)	S(4)–Re(2)–S(4')	87.37(6)
S(1)–Re(1)–S(2)	108.77(4)	S(3)–Re(2)–S(4)	109.29(4)
S(1)–Re(1)–S(2')	88.95(4)	S(3)–Re(2)–S(4')	89.31(4)
S(1)–Re(1)–P(1)	83.14(4)	S(4)–Re(2)–P(2)	82.58(4)
S(1)–Re(1)–P(1')	164.23(4)	S(4)–Re(2)–P(2')	163.95(4)
S(1')–Re(1)–S(2)	88.95(4)	S(3')–Re(2)–S(4)	89.31(4)
S(1')–Re(1)–S(2')	108.77(4)	S(3')–Re(2)–S(4')	109.29(4)
S(1')–Re(1)–P(1)	164.23(4)	S(4')–Re(2)–P(2)	163.95(4)
S(1')–Re(1)–P(1')	83.14(4)	S(4')–Re(2)–P(2')	82.58(4)
S(2)–Re(1)–S(2')	155.82(5)	S(3)–Re(2)–S(3')	154.58(5)
S(2)–Re(1)–P(1)	82.45(4)	S(3)–Re(2)–P(2)	82.29(4)
S(2)–Re(1)–P(1')	83.54(4)	S(3)–Re(2)–P(2')	83.17(4)
S(2')–Re(1)–P(1)	83.54(4)	S(3')–Re(2)–P(2)	83.17(4)
S(2')–Re(1)–P(1')	82.45(4)	S(3')–Re(2)–P(2')	82.29(4)
P(1)–Re(1)–P(1')	108.83(5)	P(2)–Re(2)–P(2')	109.77(5)

Primed labels refer to the symmetry operation: $\frac{3}{2} - x, y, 2 - z$.

co-ordinated species with a pendant SH group. This is in contrast with some recent work on the co-ordination chemistry of $Ph_2PC_6H_4S$-2 with Re^{III} where the PS ligand in $[Re\{PPh_2(C_6H_4S\text{-}2)\}_3(NCMe)(PPh_3)]$ appears to be ligated only *via* sulfur.[17] It is not entirely clear why the H_2L^2 ligand favours complete loss of the SH protons with co-ordination of all four sulfurs and formation of Re^{IV}, but it may reflect the greater acidity of the aromatic SH group and the rigidity of the aromatic backbone.

Synthesis and properties of other complexes. When the rhenium(v) precursor $[ReOCl_3(dppe)]$ (dppe = Ph_2PCH_2-CH_2PPh_2) is treated with H_2L^2 in methanol under reflux a dark purple air-stable product is formed. However, this product is *diamagnetic* and shows a singlet in the ^{31}P NMR spectrum indicating the presence of equivalent P donor atoms. The complex analyses as the rhenium(v) species $[ReL^2_2Cl]$ **14** and is a non-electrolyte in dichloromethane solution. We were unable to obtain a definitive FAB mass spectrum or to grow crystals suitable for an X-ray study.

The rhenium(vii) bis(hydrazide) complex $[ReCl_2(NNMe\text{-}Ph)_2(PPh_3)]^+$[15] reacted with a slight excess of H_2L^2 in methanol under reflux to give the orange air-stable cation $[ReL^2_2$-$(NNMePh)]^+$ **15** isolated as a BPh_4 salt. The ^{31}P NMR spectrum shows a singlet at δ 37.2 indicative of equivalent P donors. The complex is formally isolectronic with the molybdenum complex discussed above, but appears to have a different structure with equivalent L^2 ligands.

The rhenium(v) imido-complex $[ReCl_3(NPh)(PPh_3)_2]$ reacted with a slight excess of H_2L^2 in toluene under reflux to give the dark green anionic complex $[ReL^2_2(NPh)]^-$ **16** which was isolated in good yield as the PPh_4 salt after extraction into methanol. The ^{31}P NMR showed a peak at δ 26.2 due to $[PPh_4]^+$ and a singlet at δ 31.5, yet again indicating equivalent P donors. A formal valence-electron count of 18 is obtained with the imide ligand functioning as a two-electron donor and therefore presumably having a bent Re–N–Ph unit. Other possibilities with non-co-ordinated phosphorus atoms and a linear Re–N–Ph unit appear much less likely.

Synthesis of $[FeL^2_2]^-$ 15

Reaction of either $FeCl_3$ or $FeCl_2\cdot4H_2O$ with 4 equivalents of H_2L^2 in methanol in the presence of NEt_3 gave a red-brown air-stable product formulated as $[NEt_3H][FeL^2_2]$ **17**. The

Mössbauer spectrum showed a doublet with an isomer shift of $\delta = 0.24$ mm s^{-1} and a quadrupole splitting of $\Delta = 1.92$ mm s^{-1}, consistent with the formulation of the complex as low-spin Fe^{III}. There was also some evidence for the presence of a small amount of an iron(ii) contaminant, presumably $[FeL^2_2]^{2-}$. Complex **17** is very insoluble, and formulations involving thiolate-sulfur-bridged oligomers cannot be entirely ruled out. However, as is shown below, the $[NEt_3H]^+$ cation does appear to confer insolubility.

Ruthenium and osmium complexes

Of H_2L^2. The precursors $[MCl_2(PPh_3)_3]$ (M = Ru or Os) with 4 equivalents of H_2L^2 in methanol gave the complexes $[NEt_3H][ML^2_2]$ (brown, M = Ru **18**; green, M = Os **19**) in good yield, although the $[NEt_3H]^+$ salts were rather insoluble. The corresponding complexes with $[NEt_4]^+$ **20** and **21** were readily soluble in dichloromethane. The conductivities of the solutions were typical of 1 : 1 electrolytes. The NMR spectra of solutions of the complexes were very broad, consistent with the paramagnetism expected for d^5 complexes of Ru^{III} or Os^{III}. In the absence of X-ray crystallographic data we assume these complexes have the same *fac* structure as that of the rhenium complex **13** which has *cis*-P atoms.

The nitrosyl $[RuCl_3(NO)(PPh_3)_2]$ with 4 equivalents of H_2L^2 in methanol under reflux in the presence of NEt_3 gave a brown complex $[RuL^2_2(NO)]$ **22** in good yield. It is moderately stable in the solid state but solutions in organic solvents turn from brown to yellow in air over 2 or 3 d.

Analogously $[RuH(Cl)(CO)(PPh_3)_3]$ reacted with H_2L^2 in methanol under reflux in the presence of NEt_3 to give a yellow complex $[NEt_3H][RuL^2_2(CO)]$ **23**. This species is stable in both the solid state and in solution, and has a molar conductivity consistent with a 1 : 1 electrolyte. The IR spectrum shows a strong IR absorption at 1920 cm^{-1} assigned to $\nu(C\equiv O)$. Only broad ^1H NMR resonances and no ^{31}P NMR spectrum were observed, consistent with Ru^{III}. The structure is again presumably analogous to that of $[MoL^2_2(CO)]$ **9**.

(*b*) **Of H_3L^3.** Reaction of $[MCl_2(PPh_3)_3]$ (M = Ru or Os) with 2.5 equivalents of H_3L^3 in methanol under reflux in the presence of NEt_3 gave complexes of stoichiometry $[NEt_3H]$-$[M(HL^3)_2]$ (M = Ru, yellow **24**; M = Os, green **25**). These are moderately stable in air, but in solution are irreversibly converted into orange, neutral '$[M(L^3_2)]$' (M = Ru **26** or Os **27**).

The complexes $[M(HL^3)_2]^-$ when freshly dissolved in $CDCl_3$ show broad ^1H NMR resonances consistent with a paramagnetic ruthenium(iii) metal centre. It is extremely unlikely that all the thiolate sulfurs are co-ordinated as this would require eight-co-ordinate Ru^V. The colours of the complexes are directly analogous to those of the L^2 complexes $[ML^2_2]^-$ **18** and **19**, and we propose a structure **B** with two pendant SH groups.

The orange neutral complexes $[M(L^3_2)]$ **26** and **27** have been described briefly in an earlier communication,[18] and we here restrict ourselves to a short recap of the crystal structure of $[Os(L^3_2)]$ **27**. A view of the structure appears in **C**. The osmium atom is co-ordinated by a hexadentate ligand generated by the linking of two L^3 ligands by two disulfide bonds. The metal is thus in formal oxidation state ii, consistent with the observed diamagnetism. The spectroscopic characteristics of the ruthenium complex **26** are similar to those of **27** and the two are assumed to have the same structure.

The nitrosyl precursor $[RuCl_3(NO)(PPh_3)_2]$ reacted with 3 equivalents of H_3L^3 in methanol under reflux in the presence of NEt_3 to give brown $[RuL^3(NO)(PPh_3)]$ **28**. It is air stable in the solid state and in solution. There is a strong IR band at 1812 cm^{-1} assigned to $\nu(NO)$. The ^1H NMR spectrum is uninformative showing only a complex multiplet in the δ 6–8

B

C

D

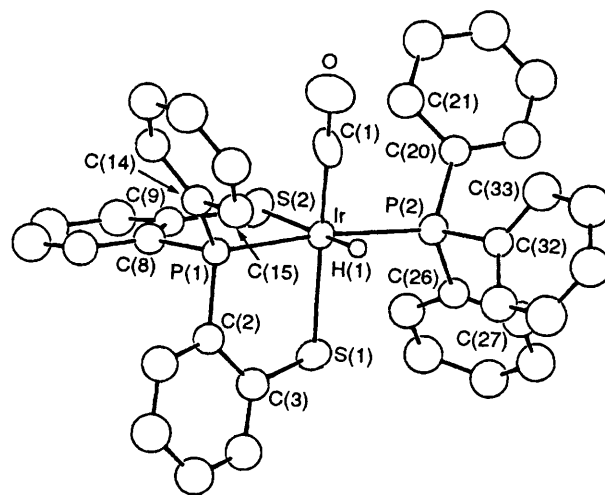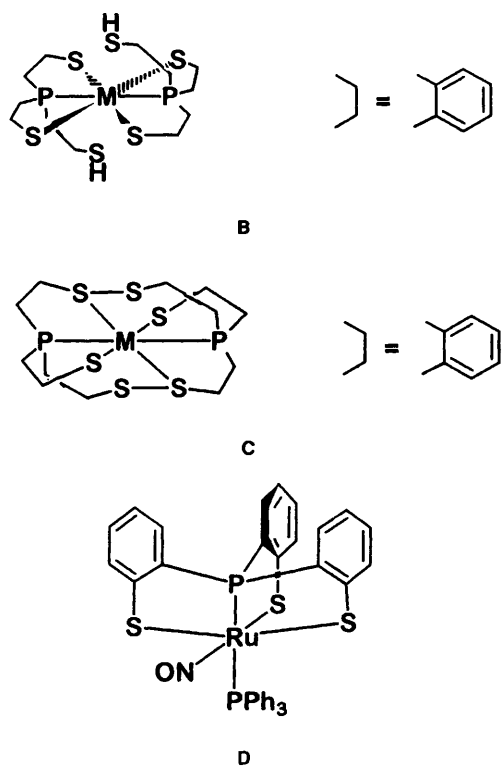Fig. 4 An ORTEP view of the structure of [IrL²(H)(CO)(PPh₃)] with the atom labelling scheme

region due to phenyl protons. However the ³¹P NMR shows two sharp doublets at δ 111.9 and 25.9 [J(P–P) = 260 Hz] in accord with the presence of two inequivalent P atoms and the coupling constant indicates a *trans* arrangement. Based on these data we assign the octahedral structure shown in **D**.

Analogous reaction of [RuH(Cl)(CO)(PPh₃)] with H₃L³ gave an insoluble yellow solid of apparent stoichiometry [RuL³(CO)(PPh₃)] **29**. The lack of solubility suggests a polymeric structure, probably with thiolate bridges, and precluded any solution spectroscopic studies.

Rhodium and iridium complexes

(*a*) **With H₂L².** Reaction of any of the precursors [RhCl(PPh₃)₃], [RhCl(CO)(PPh₃)₂], [RhCl₂(NO)(PPh₃)₂] or [IrCl₃(PMePh₂)₃] with 4 equivalents of H₂L² in methanol under reflux in the presence of NEt₃ gave complexes of the type [NEt₃H][ML²₂] (M = Rh, orange **30**; M = Ir, yellow **31**). These complexes are relatively insoluble, as observed for other [NEt₃H]⁺ salts, but the corresponding [NBuⁿ₄]⁺ salts (Rh **32** or Ir **33**) are readily soluble in solvents such as dichloromethane. All the complexes are stable in air in both the solid state and solution. Complexes **30** and **31** are not sufficiently soluble for NMR studies. The ¹H NMR spectra of **32** and **33** show the expected resonances for the Buⁿ group and ligand phenyl protons. The ³¹P NMR spectrum of **32** shows a doublet at δ 77.9 with a Rh–P coupling constant of 104.1 Hz. The corresponding iridium complex **33** shows a singlet at δ 48.0 also consistent with equivalent P donors. It is probable that all the complexes have a structure analogous to that of the rhenium complex **13**.

The precursor [IrCl(CO)(PPh₃)₂] reacted with an excess of H₂L² under similar conditions to those described above to give the white complex [IrL²(H)(CO)(PPh₃)] **34** which is air stable both in the solid state and solution. The IR spectrum shows a strong band at 2032 cm⁻¹ assigned to ν(C≡O) and a weak, sharp band at 2110 cm⁻¹ due to ν(Ir–H). The ¹H NMR spectrum in CDCl₃ exhibited a triplet at δ −11.3 with a P–H coupling constant of 11.7 Hz. This would be consistent with a *cis* arrangement of P atoms with both having the same coupling

constant to H although inequivalent. The ³¹P NMR spectrum comprises two doublets at δ 5.8 and 59.5 [J(P–P) = 298 Hz] consistent with inequivalent *trans* phosphorus atoms.

Crystal structure of complex **34.** An ORTEP representation of the structure is shown in Fig. 4 with a partial atom labelling scheme. Table 6 gives the positional parameters, and selected bond lengths and angles are in Table 7. The geometry about Ir is approximately square pyramidal with the metal atom lying close to the P(2)S(1)C(1)P(1) plane and S(2) in the apical site. The H atom was not located in the structure, but presumably it is in the vacant site *trans* to S(2). This is consistent with the observed ¹H and ³¹P NMR spectra. The L² ligand has a facial configuration as has been found in the other structures discussed above.

(*b*) **With H₃L³.** Reaction of [IrCl(CO)(PPh₃)₂] with an excess of H₃L³ under the conditions used above gives a white complex formulated as [Ir(HL³)H(CO)(PPh₃)] **35**. It is air stable in both the solid state and solution. The IR spectrum shows bands at 2110 and 2032 cm⁻¹ assigned to ν(Ir–H) and ν(C≡O) respectively. A weak sharp band at 2567 cm⁻¹ is assigned to SH. Coupled with the similarity of the ³¹P NMR spectrum to that of **34, 35** has an analogous structure with a HP₂S₃ co-ordination sphere and one unco-ordinated SH group.

The reaction of [RhCl(PPh₃)₃] with an excess of H₃L³ in methanol under reflux in the presence of NEt₃ gives a yellow complex of apparent stoichiometry [NEt₃H][Rh(HL³)₂] **36** based on analysis. The IR spectrum shows a small band at 2587 cm⁻¹ assigned to ν(S–H). The ¹H NMR spectrum exhibited the resonances expected for the [NEt₃H]⁺ cation and a broad singlet at δ 4.3 was assigned to the SH protons. The ³¹P NMR spectrum showed a doublet due to the equivalent phosphorus atoms coupled to Rh. These data are entirely consistent with a structure analogous to that proposed for [Ru(HL³)₂] with two pendant unco-ordinated thiolate groups. Complex **36** oxidises rapidly in solution in air to give an orange diamagnetic complex analysing as [Rh(L³₂)]Cl **37** presumably with an analogous hexadentate ligand involving two disulfide linkages.

The reaction of [IrCl₃(PMePh₂)₃] with H₃L³ is difficult to interpret. A yellow product of apparent stoichiometry '[NEt₃H]₂[Ir(L³₂)]' is formed in good yield. The ³¹P NMR spectrum (four doublets) suggests that this product is possibly a mixture of diamagnetic complexes, but despite repeated attempts these could not be separated and satisfactorily characterised.

Table 6 Positional parameters for [IrL²(H)(CO)(PPh₃)] **34**

Atom	x	y	z	Atom	x	y	z
Ir	0.767 34(2)	0.047 91(3)	0.215 73(3)	C(16)	0.880 3(7)	0.180 5(8)	−0.142 8(8)
S(1)	0.647 0(1)	−0.027 0(2)	0.225 0(2)	C(17)	0.952 2(7)	0.151 8(9)	−0.173 6(9)
S(2)	0.817 7(2)	−0.099 2(2)	0.284 6(2)	C(18)	0.978 3(6)	0.066 8(8)	−0.139 7(8)
P(1)	0.793 8(1)	−0.030 0(2)	0.061 1(2)	C(19)	0.929 6(6)	0.006 6(8)	−0.071 4(8)
P(2)	0.726 3(1)	0.128 6(2)	0.374 5(2)	C(20)	0.796 9(5)	0.146 2(7)	0.452 4(7)
O	0.909 8(5)	0.162 7(6)	0.167 4(7)	C(21)	0.867 4(6)	0.106 9(8)	0.423 9(8)
C(1)	0.854 7(7)	0.117 9(7)	0.189 4(8)	C(22)	0.920 8(7)	0.120 3(9)	0.485 1(9)
C(2)	0.708 4(5)	−0.053 2(7)	0.018 7(7)	C(23)	0.903 4(7)	0.175 2(9)	0.571 7(9)
C(3)	0.643 3(5)	−0.054 7(7)	0.097 3(7)	C(24)	0.834 9(7)	0.213 9(9)	0.599 5(9)
C(4)	0.578 1(6)	−0.082 2(8)	0.069 0(8)	C(25)	0.780 5(7)	0.201 8(8)	0.542 6(8)
C(5)	0.574 7(6)	−0.107 3(8)	−0.029 3(8)	C(26)	0.650 5(5)	0.070 9(6)	0.465 2(7)
C(6)	0.637 3(7)	−0.106 4(8)	−0.106(1)	C(27)	0.596 8(6)	0.128 5(8)	0.528 2(8)
C(7)	0.703 7(6)	−0.077 7(8)	−0.079 6(8)	C(28)	0.544 5(7)	0.082 3(8)	0.604 2(9)
C(8)	0.831 1(5)	−0.149 5(7)	0.079 9(7)	C(29)	0.545 5(7)	−0.016 1(8)	0.617 7(9)
C(9)	0.838 6(5)	−0.176 6(7)	0.175 9(7)	C(30)	0.597 1(7)	−0.073 2(8)	0.555 8(9)
C(10)	0.861 3(6)	−0.273 4(8)	0.190 8(8)	C(31)	0.649 9(6)	0.027 5(7)	0.479 8(8)
C(11)	0.879 7(7)	−0.337 3(9)	0.108 4(9)	C(32)	0.689 3(5)	0.249 0(7)	0.353 5(7)
C(12)	0.873 6(7)	−0.307 4(8)	0.013 4(9)	C(33)	0.723 9(7)	0.334 9(8)	0.371 3(8)
C(13)	0.849 7(6)	−0.213 7(8)	−0.003 6(8)	C(34)	0.690 9(8)	0.427(1)	0.349(1)
C(14)	0.855 5(5)	0.034 1(7)	−0.040 5(7)	C(35)	0.629 4(7)	0.428 0(9)	0.311(1)
C(15)	0.831 4(6)	0.121 0(8)	−0.077 7(8)	C(36)	0.596 5(7)	0.343(1)	0.292(1)
				C(37)	0.626 6(6)	0.253 2(8)	0.310 2(8)

Table 7 Selected bond lengths (Å) and angles (°) for complex **34**

Ir–S(1)	2.411(3)	Ir–C(1)	1.84(1)
Ir–S(2)	2.459(3)	C(1)–O	1.17(1)
Ir–P(1)	2.283(2)	S(1)–C(3)	1.76(1)
Ir–P(2)	2.371(3)	S(2)–C(9)	1.771(9)
S(1)–Ir–S(2)	92.4(1)	S(2)–Ir–P(2)	96.98(9)
S(1)–Ir–P(1)	83.01(9)	S(2)–Ir–C(1)	96.7(4)
S(1)–Ir–P(2)	91.43(9)	P(1)–Ir–P(2)	173.84(9)
S(1)–Ir–C(1)	169.6(4)	P(1)–Ir–C(1)	92.7(3)
S(2)–Ir–P(1)	85.94(9)	P(2)–Ir–C(1)	92.3(3)
Ir–S(1)–C(3)	104.5(3)	Ir–S(2)–C(9)	102.5(3)
Ir–P(1)–C(2)	108.9(3)		

Conclusion

The tridentate proligand H_2L^2 forms octahedral complexes $[ML^2_2]^{n-}$ ($n = 0$ or 1) with a wide range of metal ions. Despite their apparent co-ordinative unsaturation and high formal oxidation state, the complexes with M = Mo, W or Re react with CO to give rare examples of d^3 and d^4 carbonyl complexes. Two distinct geometries are adopted for seven-co-ordinate complexes of general type $[ML^2_2X]^{n-}$ ($n = 0$ or 1) where X can be neutral donors such as MeCN, CO or NO or the multiply bonded nitrogen ligands NPh or NNMePh. One geometry involves equivalent P atoms and in the other they are inequivalent. There is no clear pattern of the dependence on the nature of X, and the final geometry must depend on the transition states involved in stepwise substitution of the precursor ligands by H_2L^2. The potentially tetradentate proligand H_3L^3 forms analogous species to those of L^2, $[M(HL^3)_2]^-$ in which one thiolate sulfur on each ligand is protonated and not co-ordinated. Oxidation by air leads to oxidative coupling of each pendant SH group with a ligated thiolate S to generate hexadentate P_2S_4 donor complexes.

Experimental

The syntheses of proligands and metal complexes were carried out under dinitrogen using conventional Schlenk techniques and all solvents were freshly distilled from appropriate drying agents prior to use. Elemental analyses were performed by S. Hodder at the University of Essex or Medac Ltd, University of Brunel. Infrared spectra were recorded as Nujol mulls (NaCl plates) on a Perkin-Elmer 1330 or FT IR spectrometer,

¹H and ³¹P-{¹H} NMR on an EX-270 JEOL (270 MHz for ¹H) spectrometer. The FAB mass spectra were recorded at the University of Essex, by E. Potter, on an MS 50 instrument or by the EPSRC at the University of Swansea facility.

The following precursors were prepared by the literature methods: [MCl₄(PPh₃)] (M = Mo or W),[19,20] [MoCl₂-(CO)₂(PPh₃)₂],[21] [ReOCl₃(PPh₃)₂],[22] [MCl₂(PPh₃)₃] (M = Ru or Os),[23] [RuCl₃(NO)(PPh₃)₂],[24] [RuH(Cl)(CO)-(PPh₃)₃],[24] [RhCl(PPh₃)₃],[25] [RhCl₂(NO)(PPh₃)₃],[24] [IrCl₃-(PMePh₂)₃][26] and [IrCl(CO)(PPh₃)₂].[27]

Preparations

[MoL²₂] 1. The proligand H_2L^2 (0.15 g, 0.46 mmol) was added to a suspension of [MoCl₄(PPh₃)₂] (0.14 g, 0.18 mmol) in methanol and the mixture heated under reflux for 2 h to give complex **1** as a dark orange-brown precipitate (0.1 g, 72%).

[WL²₂] 2. This complex was prepared similarly to **1** as a dark green solid in 56% yield.

[MoL²₂(NCMe)] 3. This complex was prepared as for **1**, from [MoCl₄(PPh₃)₂] and H_2L^2, but using MeCN as the reaction solvent, as an orange-brown microcrystalline solid in 69% yield.

[WL²₂(NCMe)] 4. This complex was prepared as for **3** as a dark green precipitate in 65% yield.

[NMe₄]₂[MoL²(CO)₃] 5. The complex [Mo(CO)₆] (0.6 g, 2.2 mmol) in acetonitrile (30 cm³) was heated under reflux for 3 h. The salt [NMe₄]₂[L²] was prepared by the addition of a concentrated solution of [NMe₄]OH (4.4 mmol) in methanol to H_2L^2 (0.73 g, 2.2 mmol) and after stirring for 5 min at room temperature the solvent was removed *in vacuo*. The yellow solution of [Mo(CO)₃(MeCN)₃] was added under nitrogen and the solution stirred at room temperature overnight. The complex precipitated as a very air-sensitive orange solid in 82% yield.

[NMe₄]₂[WL²(CO)₃] 6. This complex was prepared similarly to **5** using [W(CO)₃(MeCN)₃], in 72% yield.

[NMe₄]₂[Mo{PMe(C₆H₄S-2)₂}(CO)₃] 7. This complex was prepared similarly to **5** from [Mo(CO)₃(MeCN)₃] and PMe(C₆H₄SH-2)₂ in 65% yield.

[MoL²₂(CO)] 9. To [MoCl₂(CO)₂(PPh₃)₂] (0.16 g, 0.21 mmol) in methanol (20 cm³) was added H₂L² (0.17 g, 0.55 mmol) and the suspension heated under reflux for 2 h. Complex **9** precipitated as a dark red-brown solid (0.1 g, 62%).

[NEt₃H][MoL²₂(NO)] 10. The compound H₂L² (0.12 g, 0.36 mmol) was added to a suspension of [NEt₃H][Mo(NO)(SPh)₄] (0.12 g, 0.15 mmol) in methanol and the mixture heated under reflux for 1 h. Complex **10** precipitated as a brown-orange solid (0.04 g, 65%).

[MoL²₂(NNMePh)] 11. The compound H₂L² (0.10 g, 0.32 mmol) was added to a suspension of [MoCl(NNMePh)₂(P-Ph₃)₂]Cl (0.15 g, 0.16 mmol) and the mixture heated under reflux for 2 h. Complex **11** precipitated as a dark brown solid, which was recrystallised from dichloromethane–methanol as brown prisms (0.09 g, 77%).

[WL²₂(NNMe₂)] 12. This complex was prepared analogously to **11** as a very dark green solid from [WCl(NNMePh)₂-(PPh₃)₂][BPh₄] (0.14 g, 0.13 mmol) in methanol (30 cm³) and the mixture stirred at room temperature for 1 h. Addition of a solution of Na[BPh₄] (0.1 g) in methanol (10 cm³) precipitated **15** as a brown-orange solid (0.11 g, 66%).

[ReL²₂] 13. The complex [ReOCl₃(PPh₃)₂] (0.12 g, 0.12 mmol) and H₂L² (0.12 g, 0.36 mmol) in methanol (30 cm³) were heated under reflux for 1 h. On cooling complex **13** precipitated as a purple solid (0.8 g, 79%) which was recrystallised from dichloromethane–diethyl ether.

[ReL²₂Cl] 14. The complex [ReOCl₃(Ph₂PCH₂CH₂PPh₂)] (0.20 g, 0.28 mmol) and H₂L² (0.19 g, 0.58 mmol) in toluene (20 cm³) were heated under reflux for 1 h. On cooling complex **14** precipitated as a purple solid in 67% yield.

[ReL²₂(NNMePh)][BPh₄] 15. The complex [ReCl₂-(NNMePh)₂(PPh₃)][BPh₄] (0.14 g, 0.13 mmol) and H₂L² (0.10 g, 0.32 mmol) in methanol (20 cm³) were stirred at room temperature for 1 h. Addition of sodium tetraphenylborate (0.1 g) precipitated complex **15** as a brown-orange solid (0.11 g, 66%).

[PPh₄][ReL²₂(NPh)] 16. The complex [ReCl₃(NPh)(PPh₃)₂] (0.22 g, 2.4 mmol) and H₂L² (0.1 g, 4.9 mmol) in toluene (20 cm³) were heated under reflux for 30 min. The toluene was removed *in vacuo* and the residue dissolved in methanol (25 cm³). Addition of PPh₄Br (0.6 g) gave the complex as a brown solid in 53% yield.

[NEt₃H][FeL²₂] 17. The compounds H₂L² (0.16 g, 0.49 mmol), FeCl₃ (0.02 g, 0.12 mmol) and NEt₃ (0.15 cm³) were heated under reflux in methanol (25 cm³) for 3 h. Complex **17** precipitated as a green solid (0.07 g, 72%).

[NEt₃H][RuL²₂] 18. This complex was prepared analogously to **17** from [RuCl₂(PPh₃)₃] and H₂L² as a brown solid in 95% yield.

[NEt₃H][OsL²₂] 19. This complex was prepared analogously to **18** from [OsCl₂(PPh₃)₃] and H₂L² as a green solid in 96% yield.

[NEt₄][RuL²₂] 20. This complex was prepared analogously to **17** from [RuCl₂(PPh₃)₃] and H₂L² using LiOMe as base. It precipitated as a green solid on addition of NEt₄Cl to the MeOH solution, in 85% yield.

[NEt₄][OsL²₂] 21. This complex was prepared analogously

to complex **20** from [OsCl₂(PPh₃)₃] and H₂L² as a green solid in 77% yield.

[RuL²₂(NO)] 22. The compounds H₂L² (0.16 g, 0.49 mmol), [RuCl₃(NO)(PPh₃)₂] (0.09 g, 0.12 mol) and NEt₃ (0.15 cm³) were heated under reflux in methanol (25 cm³) for 3 h. Complex **22** precipitated as a white solid which was recrystallised from dichloromethane–methanol (0.08 g, 85%).

[NEt₃H][RuL²₂(CO)] 23. The compounds H₂L² (0.16 g, 0.49 mmol), [RuH(Cl)(CO)(PPh₃)₃] (0.11 g, 0.12 mmol) and NEt₃ (0.15 cm³) were heated under reflux in methanol (25 cm³) for 3 h. Complex **23** precipitated· from solution as a white solid (0.97 g, 75%).

[NEt₃H][Ru(HL³)₂] 24. The compounds H₃L³ (0.17 g, 0.49 mmol), [RuCl₂(PPh₃)₃] (0.11 g, 0.12 mmol) and NEt₃ (0.15 cm³) were heated under reflux in methanol (25 cm³) for 3 h. Complex **24** precipitated as a brown solid (0.09 g, 83%). Recrystallisation in air from dichloromethane–methanol gave orange [Ru(L³₂)] **26** in high yield.

[NEt₃H][Os(HL³)₂] 25. This complex was prepared analogously to **24** from H₃L³ and [OsCl₂(PPh₃)₃]. Recrystallisation from dichloromethane–methanol in air gave air-stable [Os(L³₂)] **27** in high yield.

[RuL³(NO)(PPh₃)] 28. The compounds H₃L³ (0.17 g, 0.49 mmol), [RuCl₃(NO)(PPh₃)₂] (0.09 g, 0.12 mmol) and NEt₃ (0.15 cm³) were heated under reflux in methanol (25 cm³) for 3 h. Complex **28** precipitated as a brown solid which was recrystallised from dichloromethane–methanol (0.07 g, 78%).

[NEt₃H][RhL²₂] 30. This complex was prepared analogously to **18** from [RhCl(PPh₃)₃] and H₂L² as a yellow solid in 87% yield.

[NEt₃H][IrL²₂] 31. This complex was prepared analogously to **18** from [IrCl₃(PMePh₂)₃] and H₂L² in methanol as a yellow solid in 81% yield.

[NBu₄][RhL²₂] 32 and [NBu₄][IrL²₂] 33. These complexes were prepared analogously to **30** and **31** by addition of NBu₄Cl to the reaction solutions, in yields of 43 and 32% respectively.

[IrL²(H)(CO)(PPh₃)] 34. The compounds H₂L² (0.17 g, 0.49 mmol), [IrCl(CO)(PPh₃)₂] (0.09 g, 0.12 mmol) and NEt₃ (0.15 cm³) were heated under reflux in methanol (25 cm³) for 2 h. Complex **34** precipitated as a white solid (0.08 g, 83%).

[Ir(HL³)H(CO)(PPh₃)] 35. This complex was prepared analogously to **34** using H₃L³, as a white solid in 60% yield.

[NEt₃H][Rh(HL³)₂] 36. This complex was prepared analogously to **24** from H₃L³ and [RhCl(PPh₃)₃] as a yellow solid in 77% yield. Recrystallisation in air from dichloromethane–methanol gave [Rh(L³₂)]Cl **37** in good yield.

Crystallography

The experimental details for the determination of the crystal structures of complexes **5**, **13** and **34** are summarised in Table 8. Graphite-monochromated Mo-Kα radiation was employed (λ = 0.710 73 Å) in each case.

[NMe₄]₂[MoL²(CO)₃] 5. *Data collection.* Intensity data were collected on an Enraf-Nonius CAD4 diffractometer. Cell constants were obtained from least-squares refinement of the

Table 8 Summary of crystal data and experimental conditions for $[NMe_4]_2[MoL^2(CO)_3]$ 5, $[ReL^2_2]\cdot Et_2O$ 13 and $[Ir(L^2)(H)(CO)(PPh_3)]$ 34*

	5	**13**	**34**
Empirical formula	$C_{29}H_{37}MoN_2O_3PS_2$	$C_{40}H_{36}OP_2ReS_4$	$C_{37}H_{29}IrOP_2S_2$
M	652.67	909.1	807.92
Colour (habit)	Orange prism	Purple prism	Light red, block
Crystal size/mm	$0.5 \times 0.5 \times 0.5$	$0.14 \times 0.14 \times 0.28$	$0.24 \times 0.25 \times 0.25$
Space group	$P2_1/n$	$P2_1/a$	$P2_1/a$
$a/Å$	10.1271(40)	18.9596(76)	18.326(4)
$b/Å$	18.0772(34)	10.8054(11)	13.626(3)
$c/Å$	17.1775(70)	19.3879(74)	13.327(3)
$\beta/°$	102.210(19)	106.982(17)	78.58(2)
$U/Å^3$	3074(3)	3798(4)	3262
$D_c/g\,cm^{-3}$	1.41	1.59	1.645
μ/cm^{-1}	6.28	35.7	43.26
$F(000)$	1352	1812	1592
T/K	291	291	296
2θ Range/°	3.0–50.0	3.0–50.0	0–55
hkl Ranges	-12 to 0, -21 to 0, -20 to 20	0–22, 0–12, -23 to 23	0–23, 0–17, -17 to 17
Reflections collected	6140	7257	8060
Reflections observed	$4209\,[F_o > 3.0\sigma(F_o)]$	$5497\,[F_o > 3\sigma(F_o)]$	$3520\,[I > 3.0\sigma(I_o)]$
Absorption correction: T_{max}, T_{min}	1.053, 0.939	1.00, 0.65	1.00, 0.65
Weighting scheme, w	$1/[\sigma^2(F_o) + (0.015F_o)^2]$	$1/[\sigma^2(F_o) + (0.01F_o)^2]$	$4F_o^2/\sigma^2(F_o^2)$
R	0.031	0.027	0.039
R'	0.044	0.032	0.044
Largest hole and peak/e $Å^{-3}$	-0.19, 0.38	-0.12, 1.06	-0.86, 1.85

* Details in common: monoclinic; $Z = 4$.

setting angles of 25 centred reflections in the range $24 < \theta < 26°$. The data were collected in the ω–2θ scan mode and three standard reflections were measured every 2 h of exposure; 9.9% loss of intensity was observed which was linearly corrected during processing. Three standard reflections were measured every 200 to check the crystal orientation. The data were corrected for Lorentz and polarisation factors. An absorption correction was made using DIFABS.[28]

Structure solution and refinement. The structure was solved using the Patterson heavy-atom method (MOLEN[29]). Remaining non-hydrogen atoms were located in subsequent cycles of Fourier-difference syntheses and least-squares refinement. Full-matrix least-squares refinement on F converged with $R = 0.031$, $R' = 0.044$, maximum (shift/error) < 0.01, and $S = 1.84$. Hydrogen atoms were added in calculated positions with $B_{eq} = 1.3\,B_{eq}$ of the attached atom; they were included in structure-factor calculations but were not refined. Neutral atom scattering factors were used.[30]

$[ReL^2_2]\cdot Et_2O$ 13. *Data collection.* The procedure was as for complex **5** except as follows: range $20 < \theta < 21°$; 0.8% loss of intensity; absorption correction applied using ψ scans of nine reflections.

Structure solution and refinement. The structure was solved and refined as for complex **5** to $R = 0.027$, $R' = 0.032$, maximum (shift/error) 0.11, and $S = 1.86$. In the last few cycles the extinction coefficient was refined.

$[IrL^2(H)(PPh_3)]$ 34. *Data collection.* Intensity data were collected on an Rigaku AFC5S diffractometer in the ω–2θ scan mode and three standard reflections were measured every 150 h of exposure. No loss of intensity was observed. The data were corrected for Lorentz and polarisation factors and an absorption correction was applied using ψ scans of five reflections.

Structure solution and refinement. The structure was solved using direct methods (TEXSAN[31]). Remaining non-hydrogen atoms were located in subsequent cycles of Fourier-difference syntheses and least-squares refinement. The Ir, S, P, O and C(1) atoms were refined anisotropically, the rest isotropically. Full-matrix least-squares refinement on F converged with $R = 0.039$, $R' = 0.044$, maximum (shift/error) 0.28, and $S = 1.63$.

Hydrogen atoms were added in calculated positions with $B_{eq} = 1.25\,B_{eq}$ of the attached atom; they were included in structure-factor calculations but were not refined. Neutral atom scattering factors were used.[30]

Complete atom coordinates, thermal parameters and bond lengths and angles have been deposited at the Cambridge Crystallographic Data Centre. See Instructions for Authors, *J. Chem. Soc., Dalton Trans.*, 1996, Issue 1.

Acknowledgements

References

1 P. J. Blower and J. R. Dilworth, *Coord. Chem. Rev*, 1987, **76**, 121; J. R. Dilworth and J. Hu, *Adv. Inorg. Chem.*, 1994, **40**, 411.
2 D. W. Stephan, *Inorg. Chem.*, 1984, **23**, 2207; J. R. Dilworth, A. Hutson and J. Zubieta, *Transition Met. Chem.*, 1994, **19**, 61; F. Tisato, F. Refosco, G. Bandoli, C. Bolzati, L. Uccelli, A. Duatti and A. Pifanelli, *Proceedings of the Fourth International Symposium on Technetium and Rhenium in Chemistry and Nuclear Medicine*, eds. M. Nicolini, G. Bandoli and U. Mazzi, SGEditorali, Padova, 1995, p. 167; D. G. Dick and D. W. Stephan, *Can. J. Chem.*, 1987, **64**, 1870; G. Schwartzenbach, *Chem. Zvesti*, 1965, **19**, 200; G. Doyle, *J. Organomet. Chem.*, 1975, **101**, 85; J. Chatt, J. R. Dilworth, J. Schmutz and J. Zubieta, *J. Chem. Soc., Dalton Trans.*, 1979, 1595; G. S. White and D. W. Stephan, *Inorg. Chem.*, 1985, **24**, 1499; M. Savignac, P. Cadiot and F. Mathey, *Inorg. Chim. Acta*, 1980, **45**, L43; E. Block, H. Kang, G. Ofori-Okai and J. Zubieta, *Inorg. Chim. Acta*, 1990, **166**, 155; J. R. Dilworth, Y. Zheng, S. Lu and Q. Wu, *Transition Met. Chem.*, 1992, **17**, 364.
3 V. K. Issleib and W. Gans, *Z. Anorg. Allg. Chem.*, 1982, **491**, 163; V. K. Issleib and D. Weinbeck, *Z. Anorg. Allg. Chem.*, 1978, **440**, 5; V. K. Issleib and W. Gans, *Z. Anorg. Allg. Chem.*, 1981, **475**, 116.
4 P. J. Blower, J. R. Dilworth, G. J. Leigh, B. D. Neaves, F. B. Normanton, J. Hutchinson and J. Zubieta, *J. Chem. Soc., Dalton Trans.*, 1985, 2647.
5 E. Block, G. Ofori-Okai and J. Zubieta, *J. Am. Chem. Soc.*, 1989, **111**, 2327; E. Block, V. Eswarakrishnan, M. Gernon, G. Ofori-Okai, C. Saha, K. Tang and J. Zubieta, *J. Am. Chem. Soc.*, 1989, **111**, 658.

6 E. Block, M. Gernon, H. Kang, G. Ofori-Okai and J. Zubieta, *Inorg. Chem.*, 1991, **30**, 1736.

7 N. de Vries, A. Davison and A. G. Jones, *Inorg. Chim. Acta*, 1989, **165**, 346.

8 J. R. Dilworth and J. Hu, unpublished work.

9 J. D. Franolic, W. Y Wang and M. Millar, *J. Am. Chem. Soc.*, 1992, **114**, 6587.

10 J. D. Franolic, M. Millar and S. Koch, *Inorg. Chem.*, 1995, **34**, 1981.

11 R. J. Smith, A. K. Powell, N. Barnard, J. R. Dilworth and P. J. Blower, *J. Chem. Soc., Chem. Commun.*, 1993, 55.

12 C. K. Johnson, ORTEP, Report ORNL-5138, Oak Ridge, National Laboratory, Oak Ridge, TN, 1976.

13 D. Sellmann, F. Grasser and F. Knoch, *Inorg. Chim. Acta*, 1992, **195**, 25.

14 P. T. Bishop, J. R. Dilworth, J. Hutchinson and J. Zubieta, *Inorg. Chim. Acta*, 1984, **84**, 45.

15 J. R. Dilworth, P. Jobanputra, S. J. Parrott, R. M. Thompson, M. McPartlin and W. Hiller, *Polyhedron*, 1992, **11**, 147.

16 J. Chatt, B. A. L. Crichton, J. R. Dilworth, P. Dahlstrom, R. Gutkoska and J. Zubieta, *Inorg. Chem.*, 1982, **21**, 2383.

17 J. R. Dilworth, C. Lu and J. R. Miller, unpublished work.

18 J. R. Dilworth, J. R. Miller and Y. Zheng, *J. Chem. Soc., Dalton Trans*, 1992, 1757.

19 A. V. Butcher and J. Chatt, *J. Chem. Soc. A*, 1970, 2652.

20 J. R. Dilworth and R. L. Richards, *Inorg. Synth.*, 1980, **20**, 118.

21 A. F. Masters, G. E. Bossard, T. A. George, R. T. C. Brownlee, M. J. O'Connor and A. G. Wedd, *Inorg. Chem.*, 1983, **22**, 968.

22 J. Chatt and G. A. Rowe, *J. Chem. Soc.*, 1962, 4019.

23 P. S. Hollman, B. R. Stephenson, and G. Wilkinson, *Inorg. Synth.*, 1970, **12**, 237; F. P. Dwyer and J. W. Hogarth, *Inorg. Synth.*, 1957, **5**, 195; G. P. Elliott, N. M. McAuley and W. R. Roper, *Inorg. Synth.*, 1989, **26**, 185.

24 N. Ahmad, J. J. Levison, S. D. Robinson and M. F. Uttley, *Inorg. Synth.*, 1973, **15**, 45.

25 J. A. Osborn and G. Wilkinson, *Inorg. Synth.*, 1967, **10**, 67.

26 Y. Zheng, Ph.D. Thesis, University of Essex, 1993.

27 K. Vrieze, J. P. Collman, C. T. Sears and M. Kubota, *Inorg. Synth.*, 1964, **7**, 102.

28 DIFABS, N. G. Walker and D. Stuart, *Acta Crystallogr., Sect. A*, 1983, **39**, 158.

29 MOLEN, An Interactive Structure Solution Procedure, Enraf-Nonius, Delft, 1990.

30 D. T. Cromer and J. T. Waber, *International Tables for X-Ray Crystallography*, Kynoch Press, Birmingham, 1974, vol. 4, Table 2.3.1.

31 TEXSAN-TEXRAY, Structure Analysis Package, Molecular Structure Corporation, Houston, TX, 1985.